JGR Space Physics

RESEARCH ARTICLE
10.1029/2021JA029270

Influence of IMF-By on the Equatorial Ionospheric Plasma Drifts: TIEGCM Simulations

Debrup Hui[1,2] **and Geeta Vichare**[1]

[1]Indian Institute of Geomagnetism, Navi Mumbai, India, [2]Ghani Khan Choudhury Institute of Engineering and Technology, Malda, India

Key Points:

- East-west component of interplanetary magnetic field (IMF-By) affects the ionospheric electrodynamics beyond polar latitudes even near equator, during southward IMF
- A strong IMF-By reduces prompt penetration electric field near equator, and the effects are stronger near sunset and sunrise terminators
- Role of IMF-By polarity is seen during disturbance dynamo, giving dawn-dusk asymmetry; meridional wind reverses on IMF-By polarity reversal

Correspondence to:
G. Vichare,
geeta.vichare@iigm.res.in

Citation:
Hui, D., & Vichare, G. (2021). Influence of IMF-By on the equatorial ionospheric plasma drifts: TIEGCM simulations. *Journal of Geophysical Research: Space Physics*, *126*, e2021JA029270. https://doi.org/10.1029/2021JA029270

Received 10 MAR 2021
Accepted 4 AUG 2021

Abstract The influence of east-west component of interplanetary magnetic field (IMF-By) on ionospheric plasma convection over polar region is well established by both observation and modeling studies. However, its influence beyond polar latitudes has rarely been addressed. To understand the effects of IMF-By at low-latitudes during geomagnetic storm times, we have designed simulation experiments using Thermosphere-Ionosphere-Electrodynamics General Circulation Model. This communication shows that strong IMF-By and its polarity has effects on the storm-time ionosphere-thermosphere dynamics even near equator. It can change zonal electric field, magnitude of morning/evening time pre-reversal-enhancements (PRE) and meridional winds. At the storm onset when prompt penetration electric fields prevail, a strong IMF-By, in general, reduces the vertical plasma drifts over the equator and the largest effects are observed near sunrise and sunset terminators. Later when disturbance dynamo is active, morning PRE appears, and a strongly positive IMF-By strengthens morning PRE and weakens evening PRE, with respect to zero IMF-By conditions. A strongly negative IMF-By just shows the reverse, thus indicates dawn-dusk asymmetry due to IMF-By. It is also seen that the meridional winds are oppositely directed during positive and negative IMF-By conditions. The effects of IMF-By transition are observed on the evening PRE within 2 h from the transition. The new insights successfully explain the observations from a few earlier available works. However, the presented results should be treated with caution in view of model limitations associated with the empirical patterns of high latitude convection and preliminary scheme of merging high latitude-low latitude potentials.

Plain Language Summary Storm time reconnection results in exchange of huge amount of momentum, energy and particles, which causes changes in the Earth's ionosphere-thermosphere system. When the primary driver north-south component of interplanetary magnetic field (IMF-Bz), controls this flow of energy and particles, east-west component of interplanetary magnetic field (IMF-By) modulates this flow thereby altering the impacts on the Earth's ionosphere during geomagnetic storm evolution. Our knowledge about this modulation is limited to polar regions only, where it is quite pronounced. The impact of IMF-By beyond polar ionosphere is sparse and has rarely been reported. This is because of the masking of its influence by the overwhelming effects of IMF-Bz. In this study, special experiments are designed using Thermosphere-Ionosphere-Electrodynamics General Circulation Model to understand the impact of IMF-By on ionosphere near equator, during storm times. It is found that a strong IMF-By during geomagnetic storm and its polarity can substantially influence the plasma convection up to equatorial latitudes and alter the neutral dynamics as well. A reliable space weather forecasting must incorporate the effects of IMF-By.

1. Introduction

The essence of space weather research for making a robust forecast model to support space-based assets lies in the good understanding of the impact of different solar wind and interplanetary drivers on the magnetospheric-ionospheric electrodynamics. The solar wind electric field ($\mathbf{E}_{sw} = -\mathbf{V}_{sw} \times \mathbf{B}_{sw}$) is the rate at which magnetic flux is carried in the solar wind toward the Earth, which depends on the solar wind velocity, strength and orientation of interplanetary magnetic field (IMF), and is considered as a driver for the solar wind-magnetosphere coupling. The solar wind electric field driver functions are expressed in various forms as $V_{sw}B\perp$ times a clock angle function, where $B\perp$ is the component of IMF perpendicular to the sun-earth line (e.g., Kan & Lee, 1979; Newell et al., 2007; Wygant et al., 1983). The north-south component of interplanetary magnetic field (IMF-Bz) is the primary driver for solar wind-magnetosphere-ionosphere

coupling. The day side reconnection due to southward turning of the IMF-Bz component and its impact on the geospace is well studied and well understood in the perspective of enhanced energy, momentum, and particle flow form solar wind to magnetosphere and their effects on the global ionosphere/thermosphere system. Over auroral region, it results in the development of two plasma convection vortexes, popularly known as DP2 (Nopper & Carovillano, 1978; Ruohoniemi & Greenwald, 2005), whereas over low to equatorial latitudes, it enhances the dayside eastward zonal electric field and induces westward electric field in the post-midnight to morning sector (Fejer et al., 2008), during almost instantaneous prompt penetration electric field (PPEF) effects. Intense and long-duration southward IMF manifests geomagnetic storms on the Earth (Gonzalez et al., 1994). The enhanced energy inputs at high latitudes during geomagnetic storm cause considerable heating, which drives the neutral winds. The disturbed neutral winds cause F region electric fields by the disturbance dynamo (DD) mechanism (Blanc & Richmond, 1980), which are opposite to the PPEFs and reach the equator after 2–3 h. The $\mathbf{E} \times \mathbf{B}$ vertical drifts over equator are considered as proxy for these zonal electric fields associated with PP/DD.

The east-west component of interplanetary magnetic field (IMF-By) is known to rotate the two-cell convection pattern in the polar ionosphere produced by the southward IMF-Bz (Ruohoniemi & Greenwald, 2005). Modifications of high latitude convection patterns, winds, thermospheric densities, hemispherical asymmetries etc., arising due to IMF-By changes have been studied, both by simulations and observations (e.g., Förster & Haaland, 2015; Immel et al., 2006; Khurana et al., 1996; Tenfjord et al., 2015; Yamazaki et al., 2015; Ohma et al., 2018). Recently Holappa et al. (2020) have reported IMF By dependence in the westward electrojet and geomagnetic activity by modulating ionospheric conductivity. They found that the IMF By effect on electron fluxes exhibits seasonal dependence, and is strong around midnight to dawn and weak at dusk. But the effect of the IMF-By beyond the polar latitudes has rarely been addressed and still remains very obscure. By now, it is well known that non-zero IMF-By component induces dawn-dusk component of the magnetic field (By) in the closed magnetosphere, however the exact mechanism of this induced component is a topic of debate (Tenfjord et al., 2015). Understanding the impact of IMF-By at lower latitude ionosphere through observations is challenging, mainly because of the overwhelming effects of IMF-Bz. Very few studies (Chakrabarty et al., 2017; Kelley & Makela, 2002; Mannucci et al., 2014) have tried to understand the impact of IMF-By on the ionospheric electrodynamics beyond polar latitudes. Kelley and Makela (2002) reported that the changes in the IMF-By might be responsible for the altered polarity of the storm time penetration electric field. They explained it by twisting of Northward Bz (NBZ; Iijima et al., 1984) current system by IMF-By. Mannucci et al. (2014) has also shown that during one of the biggest magnetic storms of solar cycle 23, the TEC did not increase as fast as in case of many similar and weaker storms. They suspected that unlike other cases, a strong IMF-By during the onset of the storm in that particular event was possibly responsible for low TEC values. Chakrabarty et al. (2017) also observed that the polarity of PPEF over two antipodal stations: Jicamarca and Thumba were found to be same when opposite directions of PPEF are expected (Kelley et al., 2007). They have suggested a mechanism of how the influence of IMF-By can affect the global ionosphere beyond rotating the polar DP2 potential distributions. Thus, it is propounded that IMF-By can at times modify the effects of southward IMF-Bz and even change the expected polarity of storm time fields up to equatorial latitudes. From the few event-based observations of large deviations from the expected PPEF, the role of IMF-By in controlling the storm time electrodynamics of global ionosphere is deemed critical for the evaluation of space weather events. As mentioned earlier, because of the presence of the primary and significant influence of IMF-Bz component, it is very difficult and rare to find suitable cases for delineating the influence of IMF-By. For overcoming this difficulty, in this communication we have tried to bring out the influence of IMF-By through controlled simulations. So far global MHD models such as BATS-R-US, Lyon-Fedder-Mobarry (LFM), GUMICS-4 etc. have been used to examine the role of IMF-By on the magnetospheric dynamics and configuration. Open Geospace General Circulation Model (OpenGGCM) which couples MHD model of Earth's magnetosphere with Coupled Thermosphere Ionosphere Model, have been used by Tenfjord et al. (2018) to simulate the response and reconfiguration time of the induced *By* in the magnetosphere. In the present paper, we wish to examine the response to IMF By at the ionospheric heights at low latitudes, and hence use of thermospheric-ionospheric general circulation models (GCMs) is required rather than magnetospheric models. CTIP, OpenGGCM, TIE-GCM are some of the established GCMs capable of simulating low latitude ionospheric dynamics, which can be responsive to the interplanetary conditions. In short, they can produce variable response to the changes in the IMF conditions.

TIEGCM has been successfully used to understand many quiet and storm time electrodynamic processes in the ionosphere (e.g., Hui & Vichare, 2019; Maute et al., 2021; Richmond et al., 2003; Richmond et al., 2015; Rodrigues et al., 2012; Vichare & Richmond, 2005). Quiet time processes like post sunset vortex (Rodrigues et al., 2012), longitudinal variation of post-sunset pre-reversal enhancement (PRE) (Vichare & Richmond, 2005) etc. are brought out successfully through TIEGCM simulations. PP and DD electric fields are the two main types of electric fields observed during storm at low latitudes, which have been reproduced and investigated by TIEGCM (Richmond et al., 2003). Shiokawa et al. (2007) used TIEGCM to model storm-time traveling ionospheric disturbance. Kwak and Richmond (2014) and Kwak et al. (2010) used TIEGCM simulations to study the effects of various IMF conditions on the high latitude thermospheric dynamics. Wang et al. (2008) used coupled magnetosphere ionosphere thermosphere (CMIT) model which uses TIEGCM to reproduce the storm time global ionospheric electric field variations. Hui and Vichare (2019) has shown that even during extremely rare occurrence of very high zonal electrical field over dip equator, as measured by highly accurate Jicamarca (11.9°S, 76.8°W; dip latitude 1°N) incoherent scatter radar, TIEGCM could closely reproduce the storm time electric field. Such studies show that TIEGCM could closely capture the quiet and disturbed time evolution of storm time electrodynamics. The present work plans to extend the study of IMF-By effects to near equatorial latitudes using TIEGCM simulations. In this study, comparing results from 3 different experiments using TIEGCM carried out at Community Coordinated Modeling Center (CCMC) brings out interesting results about the influence of IMF-By on equatorial electrodynamics during various phases of the geomagnetic storm. This is for the first time GCM simulations have been used to investigate the IMF-By effects at the equator. The designed simulations allow the study of these effects on PPEF and disturbance dynamo electric field (DDEF). The occurrence of evening PRE which is a post-sunset enhancement of eastward electric field before turning westward at night, is a regular feature observed over the equator. While similar feature near sun-rise terminator, called as morning PRE is not a regularly observed feature. Present work reveals varying effects of IMF-By on PPEF, DDEF, evening PRE and morning PRE.

This paper has been arranged in the following sequence: First, the specifications and limitations of TIEGCM are described. Next the depiction of the three TIEGCM experiments carried out is given. This is followed by the results which discuss the influence of IMF-By and its transition on the local time pattern including evening PRE, during various phases of the storm. The paper ends with the discussion and summary.

2. Description of TIEGCM

The NCAR TIE-GCM is a general circulation model which solves full three-dimensional momentum, energy and continuity equations for numerous neutral and ion species. TIEGCM is a comprehensive, first principles, non-linear representation of the coupled thermosphere-ionosphere system with a self-consistent solution of the low-latitude electric field, which gives low-latitude plasma drifts as one of the outputs. The low-to-mid latitude wind dynamo is solved to provide global electric potential. For the time scales of a minute and longer, the assumption of equipotential field lines holds and the hemispheric differences in the wind dynamo generate inter-hemispheric current at low-middle latitudes. The default simulation settings for the model are 5° × 5° latitude-longitude grid size and 29 constant pressure levels in the vertical direction covering from 97 to about 500 km. The model considers particle precipitation and daily F10.7 solar index along with 81-day averaged F10.7 index. The upper boundary conditions for electron heat transfer and electron number flux are empirical formulations. In the present work, the simulations used the default 5° × 5° latitude-longitude grid size and the output plasma drifts are obtained with a temporal resolution of 5 min. The ionospheric electric potentials at high latitudes are derived from Weimer (2005) ion convection model, which is based on the Dynamic Explorer 2 data set. The IMF components (IMF-By, IMF-Bz), solar wind density and speed (Vsw) go as inputs. The ion convection pattern and the Cross Polar Cap Potential (CPCP) are very sensitive to IMF Bz, IMF By, and Vsw. Interhemispheric asymmetry in this model is simplified by reversing the signs of IMF By and Earth's dipole tilt angle. Even with this simplification, Weimer model has been useful in understanding the general behavior of the thermosphere-ionosphere system (Lei et al., 2015; Qian et al., 2014). However, it is known that the high latitude potential patterns in the north and south hemispheres are not symmetric during times of significant IMF By. The potential pattern in the northern hemisphere for positive IMF By conditions resembles with that in the southern hemisphere for negative IMF By, and vice versa (Förster & Haaland, 2015). In TIEGCM, the sign of IMF By is changed for the potential

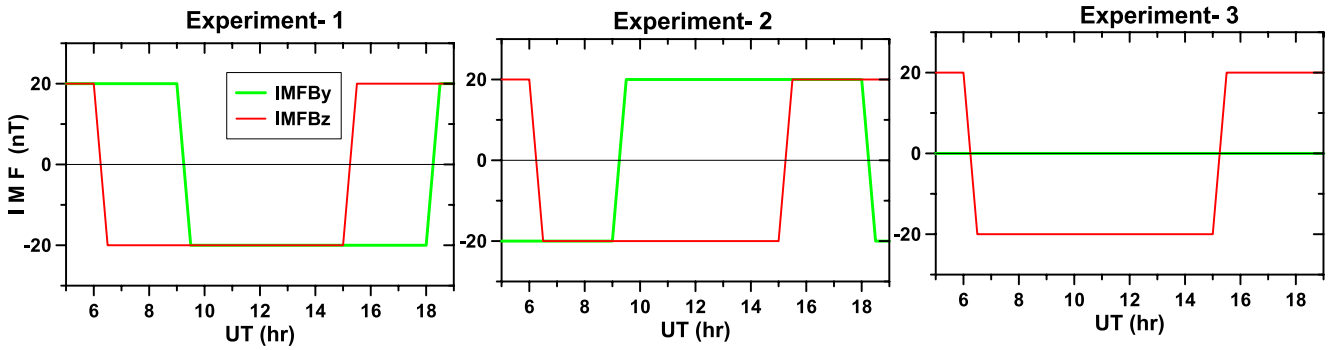

Figure 1. Interplanetary magnetic field conditions during three Thermosphere-Ionosphere-Electrodynamics General Circulation Model simulation experiments.

pattern in the southern hemisphere. This makes similar patterns in both the hemispheres, and hence there could be hemispheric symmetry in those patterns. Thus, the middle and low latitude potential pattern in the model is asymmetric, while the high latitude pattern can be different. This may put constraints on the model results due to non-consideration of the inter-hemispheric asymmetries in high latitude potential patterns. Recently, Maute et al. (2021) used new approach to prescribe observed field aligned currents in TIEGCM to solve for inter-hemispherically asymmetric electric potentials at high latitudes. They found it useful in improving the temporal variation, compared to empirical models of high latitude potentials.

In TIEGCM, the region of the wind dynamo is merged with the high latitude region at a cross-over boundary, which varies dynamically with the strength of the magnetospheric forcing (Maute, 2017). This merging region extends over a 15° latitude range, between 60° and 75° geomagnetic latitude, where a linear variation of the combined dynamo solution and the imposed high latitude solution is considered. It may be possible that with this preliminary merging scheme, the leakage of high latitude changes into the low latitudes may not be realistic, however this needs to be examined with observations.

The ion velocities are derived from the potential field created by combining the imposed magnetospheric potential with the low-latitude dynamo potential, and then calculating ion velocities from E × B drifts, rather than solving the ion momentum equations explicitly. At the bottom side boundary, it takes diurnal and semidiurnal migrating tides specified by Global Scale Wave Model (GSWM; Hagan & Forbes, 2002). More details about the model can be obtained from Dickinson et al. (1981), Qian et al. (2014), Roble et al. (1988), and Richmond et al. (1992), and references therein. The geomagnetic coordinates used here are obtained using APEX geomagnetic coordinate (Richmond, 1995).

The model response to the IMF By drivers seen through the equatorial PPEF and DDEF are presented in this paper. We present our results with a caveat that the method used in the model to calculate the merging of high latitude potential with low to middle latitude wind dynamo potential is preliminary and non-consideration of hemispherically asymmetric potentials at high latitudes may affect the results. This may put a limitations on the results presented in this paper.

3. TIEGCM Simulations

TIEGCM simulation runs are made at CCMC for three different solar wind conditions of varying IMF-Bz and IMF-By. The solar wind velocity of 450 km/s is used throughout the simulations. Figure 1 sketches the transitions of IMF-Bz and IMF-By customized during three simulations. In all the three runs, the temporal variations of IMF-Bz are kept the same, which are as follows: at 0600 UT IMF-Bz makes a transition from +20 nT (northward) to −20 nT (southward) over a period of 30 min from 0600 to 0630 UT; and after about 9 h at 1500 UT it turns northward (+20 nT) in 30 min time interval. In the first simulation (Figure 1a), the transition of IMF-By is performed from positive (dusk-ward) to negative (dawn-ward) under southward IMF-Bz condition. Accordingly, at 0900 UT, IMF-By makes a transition from +20 nT to −20 nT over 30 min. The 2.5-hour gap is designed intentionally to minimize the mixing of the sudden impact from PPEF due to southward IMF-Bz turning with the effects of IMF-By changes. Also, it is normally considered that the

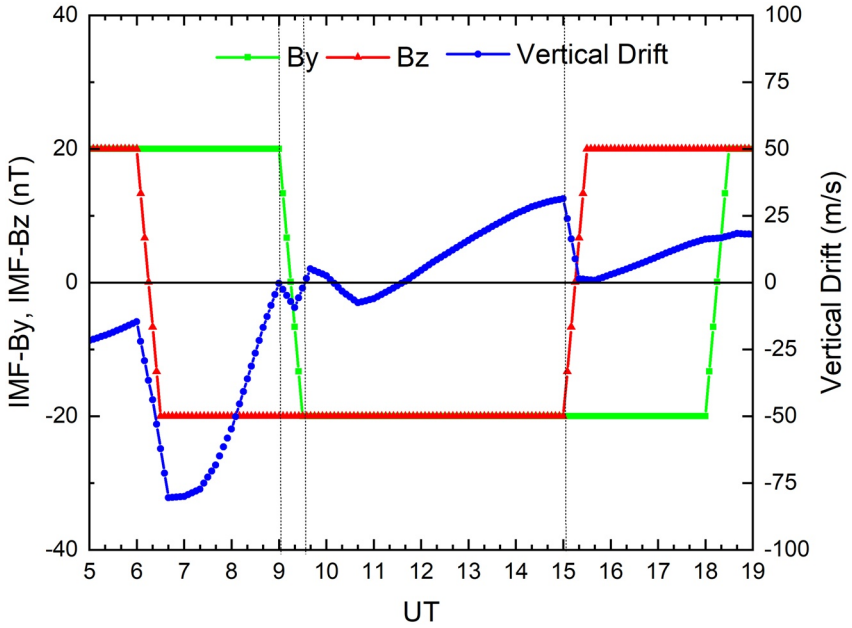

Figure 2. Vertical plasma drifts at 350 km altitude obtained over Jicamarca through the first Thermosphere-Ionosphere-Electrodynamics General Circulation Model simulation.

disturbance dynamo effects are evident after about 2–3 h of IMF-Bz turnings. So, soon after 0930 UT when IMF-By has turned negative, we may expect to see mostly the effects of IMF-By transition and lesser influence from PPEF and DD. At 1500 UT, when IMF-Bz turns northward, it would produce the overshielding effects. Then after 3 h, at 1800 UT IMF-By makes a transition to duskward (positive) direction. The second simulation shown in Figure 1b performs IMF-By transitions opposite to those in the first simulation that is, from −20 nT to +20 nT at 0900 UT and reverse at 1800 UT. The third simulation (Figure 1c) does not have any IMF-By transitions, thus the third experiment (Exp-3) is designed to evaluate the changes purely related to IMF-Bz only. Note that in all these simulations, we have fixed the peak amplitude of IMF-By and IMF-Bz to 20 nT, which normally occur during intense storm times. Thus, the considered IMF values assures the significant disturbance. The vertical drifts over Jicamarca in the F-region (at 350 km altitude) derived from the first TIEGCM simulation are shown in Figure 2. It can be seen that the vertical drifts respond to the sudden variations of IMF-Bz as expected for PPEF that is, when IMF-Bz turns southward at 0600 UT, the drifts over Jicamarca which is on the night side show sudden increase in the downward drifts; and when IMF-Bz turns northward at 1500 UT, the amplitude of upward drifts drops. It is also interesting to note that the drifts respond to the IMF-By changes during southward IMF, but no response during northward IMF. The detailed response from these simulations will be discussed in the next section.

4. Results

The temporal profiles of the vertical plasma drifts over geomagnetic equator in the F- region at the height of 350 km obtained from Experiment-1 and Experiment-2 at different longitudes are shown in blue in Figures 3 and 4 respectively. The vertical plasma drifts for Experiment-3 at different longitude sectors are shown by magenta curve in both Figures 3 and 4 for the comparison purpose. Both Figures 3 and 4 show drifts at different longitudes at intervals of 30° (equivalent to 2 h local time difference). The latitude, longitude and corresponding local time are mentioned on top of each panel. Note that the geographic coordinates (latitude and longitude) represent the geomagnetic equator. The IMF turnings are shown by red and green colors. The sudden change in the drift values soon after southward turning of IMF-Bz at 0600 UT can be seen in all longitude sectors, which are related to PPEF. Note that both the curves (blue and magenta) experience the same IMF-Bz changes and hence both the curves show sudden changes at 0600 UT. This PPEF related enhancement in the vertical plasma drifts (i.e., eastward electric field) in the day side (0°–210°E) and decrease in vertical drifts (i.e., westward electric field) at night side longitudes (240°E–330°E) agree

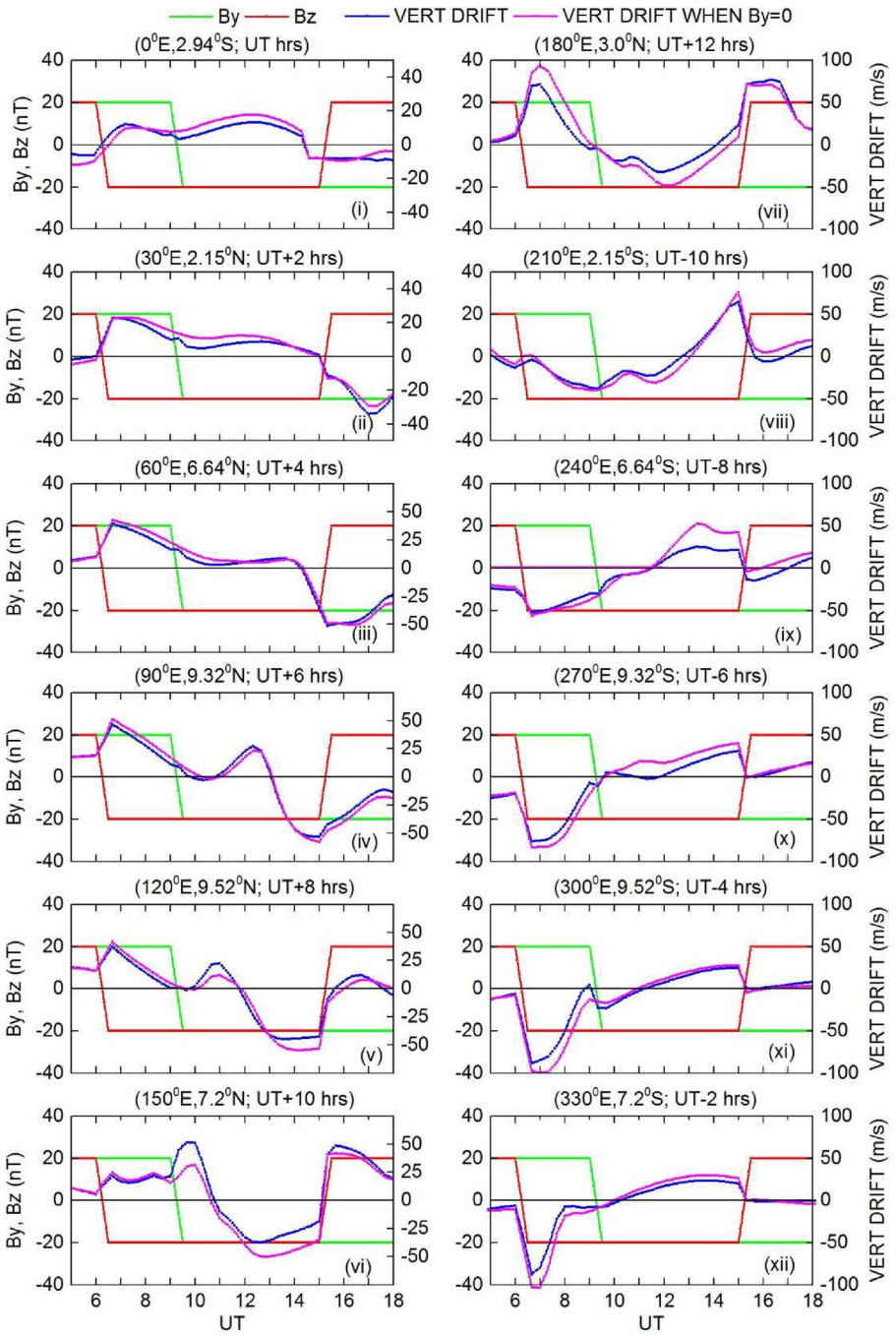

Figure 3. F-region vertical plasma drifts over magnetic equator under variable interplanetary magnetic field (IMF) conditions, at different longitudes, obtained from Experiment 1 and 3. Drifts are shown in blue when east-west component of interplanetary magnetic field (IMF-By) makes a transition as shown in green, and in magenta when IMF-By remains zero. North-south component of interplanetary magnetic field is shown in red.

well with the observations of local time variations of PPEF reported by Fejer et al. (2008). The hump seen at 180°E, at ~0700 UT in both Figures 3 and 4 represents PRE under PPEF effect, and it can be noted that the effect of IMF-By in reducing its amplitude is considerable over there. At the longitudes from 90°–150°E, a bump near local sunset hours (~0900–1300 UT) represents PRE under southward IMF-Bz conditions, but after IMF-By transition, which is about 3 h after IMF-Bz transition. At 0900 UT, when IMF-By makes a transition, the drifts (blue) show small deviation in most of the panels except in the panels of 120°–210°E

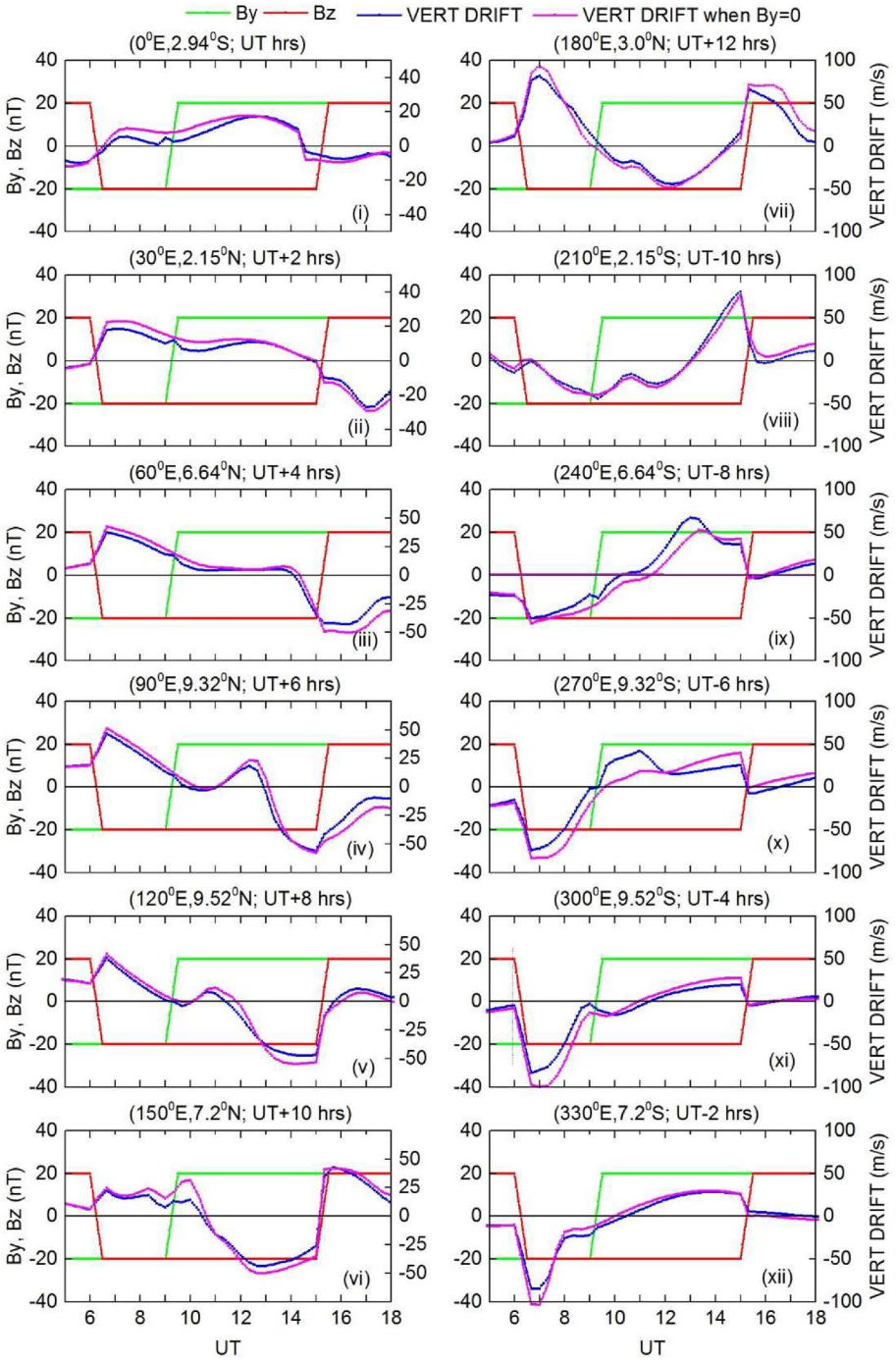

Figure 4. Same as Figure 3, but the results are from Experiment 2 and 3.

longitude which represent dusk-to-midnight sector at 0900 UT. It can be seen that during steady southward IMF-Bz conditions (0900–1500 UT), IMF-By = 0 case (magenta color) gives larger drift values in general compared to those during strongly positive or negative IMF-By conditions, except during local PRE hours which will be discussed later in the next sub-section. Present results of smaller drifts in Experiment-1 and 2 suggest weaker penetration electric fields during strong IMF-By. This may be consistent with the observations of Mannucci et al. (2014). They observed the absence of quick increase in dayside TEC for the storm on November 20, 2003 with "exceptionally large IMF-By" during storm onset when compared to many similar or even weaker storms. However the scenario at the evening PRE time is different (e.g., at 120°E and 150°E

in Figure 3). Other than evening PRE hours, another exception can be seen in Figure 4, at 240°E and 270°E near 1300 and 1100 UT respectively, which is suggested to be related to morning PRE and will be discussed later in sub-Section 4.2.

4.1. Effects on Evening PRE

The longitudes from 60°E to 180°E have evening local times during storm conditions between 0600-1500 UT. In Figures 3 and 4, a weak PRE peak is seen at ∼1400 UT at 60°E, but 90–180°E longitudes show very clear and distinct PRE peaks (0600–1300 UT). The difference in the PRE peaks seen in the blue and magenta curves is not much for 60°–90°E, when PRE is at ∼1200–1300 UT, that is, far away from IMF-By transitions at 0900 UT. But at 150°E this difference is larger, when PRE peak is at 1000 UT that is, close to the IMF-By transition. In Figure 3, even near 11 UT at 120°E, a difference of ∼5 m/s is seen, thus it appears that the PRE drifts during non-zero IMF-By conditions deviate from those of zero IMF-By conditions when PRE occurs within ∼2 h from the IMF-By transition. Also, very interesting thing one can notice is that at 150°E longitude, where PRE is at 1000 UT, non-zero IMF-By in Figure 3 shows higher drifts and that in Figure 4 shows smaller drifts than the zero IMF-By conditions. That means when the IMF-By transition is from positive to negative then the PRE peaks are stronger and when transition is from negative to positive, then the PRE peak is smaller than no transition of IMF-By with zero value. At 180°E (PRE at 0700 UT, where effects of PPEF can prevail), the PRE drift with positive IMF-By component is smaller by ∼10 m/s (Figure 3) and PRE with negative IMF-By is smaller by ∼5 m/s (Figure 4) than that of zero IMF-By conditions. This means that the PRE peak drift values are higher during negative IMF-By than that during positive IMF-By, but both these conditions show smaller drifts than zero IMF-By conditions. One can observe that in addition to PPEF and PRE peaks, there are multiple peaks (e.g., at 150°E). It is important to note that the multiple peaks do not appear because of IMF-By as they are present in magenta curves too when IMF-By = 0. The period of multiple peaks from 0500–1200 UT is being investigated and is zoomed in Figure 5, at longitudes separated by 7.5°, along with TIEGCM derived meridional winds over the equator (shown by orange curve) obtained during Experiment-3 that is, without IMF-By transitions. The first peak at ∼0645 UT (indicated by thin vertical line) is common in all panels and is due to the PPEF. The PRE peaks are shown with dashed lines, which have been identified by following the peak values of the drifts at ∼1800–1900 LT. As mentioned above, this peak is seen clearly in the bottom four panels (150°−172.5°E) in Figure 5. At 135° and 142.5°E (top two panels of Figure 5) the PRE peaks are not very clear and seems to be combined with third peak. The presence of a third broad peak (shown by thick solid lines) which is pronounced from 142.5° to 172.5°E is very interesting and intriguing. This peak is present even in magenta curve, that means it is not related to the strong IMF-By or its transition conditions. The time of this peak is found to vary between 0900-1000 UT. A clue to decipher this broad peak may come from a look at meridional winds over equator shown in orange for the case of IMF-By = 0 (experiment 3). Note that the broad peak largely coincides with the increase of the meridional winds almost after 3 h from the storm onset (PPEF at ∼0645 UT). This is being interpreted as a result of disturbance dynamo winds. Though DDEF is expected to be eastward (positive enhancement in vertical drifts) during night after sunset, Fejer et al. (2008) have suggested that in general DD generates an enhancement in the vertical drifts after 2200 LT. In this case it seems, the enhancement appeared after about 3 h of IMF-Bz transition in the post sunset sector (after ∼1900 LT). During daytimes near 09–10 UT (e.g., 0–90°E in Figures 3 and 4), this peak related to DD is absent, as during day time DD is expected to reduce the drifts. It is to be noted that the PRE peak at 120°E (in Figures 3 and 4) and 135°E and 142.5°E (in Figure 5) coincide with this broad peak and is thus difficult to separate out. Another interesting observation form Figure 5a is that when IMF-By transition is from positive to negative, the third broad peak (which is suggested to be due to DD effects) is larger than IMF-By = 0 case (panels (i–iv)). Whereas in Figure 5b, when IMF-By turns from negative to positive, the third peak is weaker than that in the magenta color. This shows that the effects of orientation of IMF-By becomes more pronounced after sometime on the DD related peak.

4.2. Effect on Local Time Pattern at Various Phases of the Storm

In the previous sub-section it was described how IMF-By affects the temporal changes around evening PRE over equatorial latitudes. It is also important to understand how the IMF-By affects the ionospheric plasma drifts at different times during disturbed conditions. These equatorial plasma drifts across all longitudes are

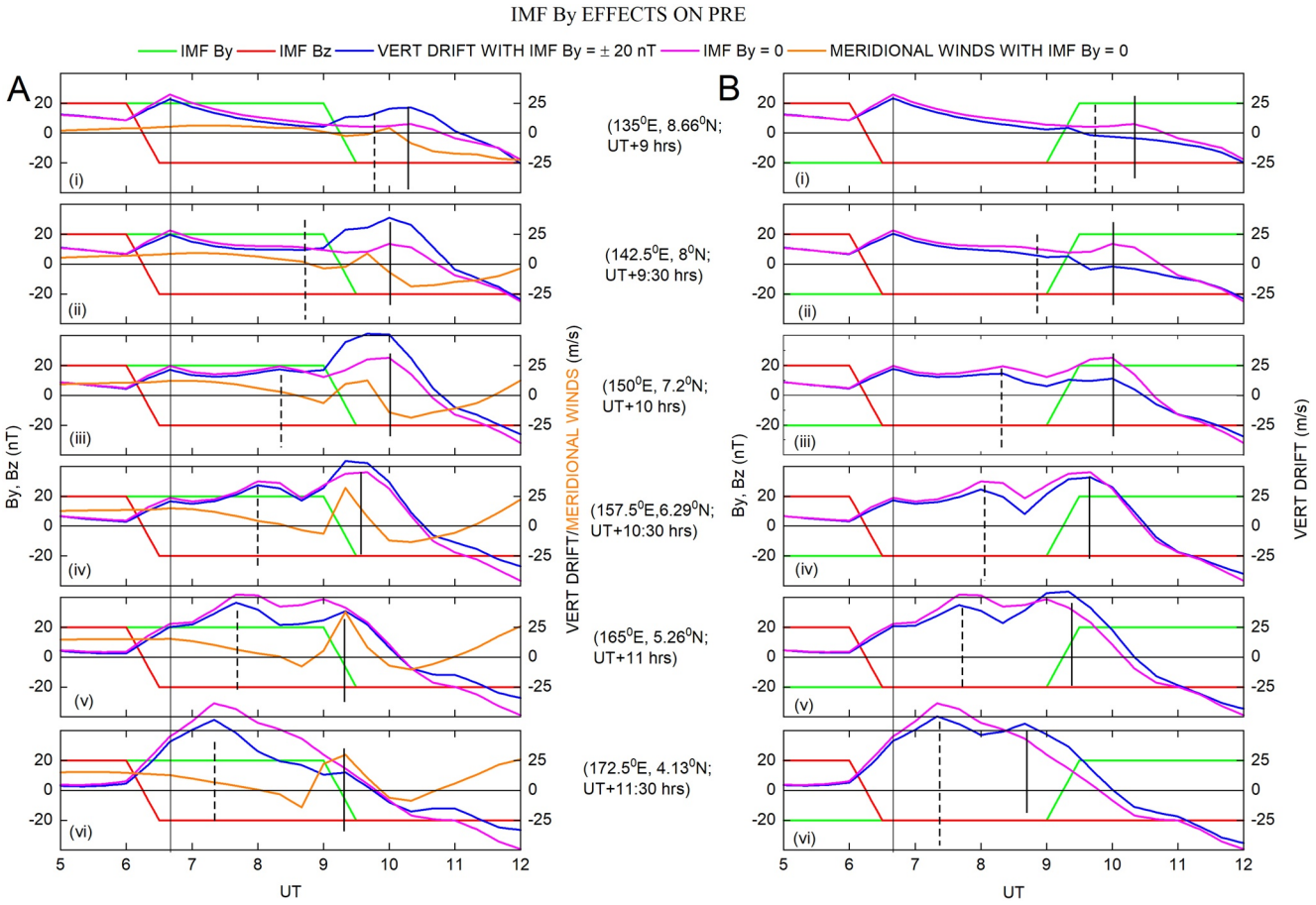

Figure 5. Evening pre-reversal enhancement (PRE) for all three experiments compared under steady southward component of interplanetary magnetic field (IMF-Bz) and influence of east-west component of interplanetary magnetic field (IMF-By) transition. Red and green lines show IMF-Bz and IMF-By transitions; blue and magenta curves show vertical plasma drifts for strong and zero IMF-By cases respectively. Orange line shows Thermosphere-Ionosphere-Electrodynamics General Circulation Model-derived meridional winds with Experiment-3, over equator. Thin vertical line just after 0630 UT indicates the enhancement due to prompt penetration electric field effect. The evening PRE time near 1800–1900 UT is shown by dashed vertical lines, and third peak is indicated by thick solid lines.

shown at different storm evolution phases in Figure 6, thus depicting snapshot at different times of storm evolution. Figure 6 shows these plots at 0500 UT (before storm), 0800 UT (into main phase but before IMF-By transition), 1000 UT (after IMF-By transition and also ~4 h after the storm onset when DD can prevail) and at 1300 and 1400 UT (well after IMF transitions when DD effects are also present). At each instant, results from all three experiments are compared to understand the effect of IMF-By. The black, green and magenta lines represent experiments 1, 2, and 3 respectively. The X-axis indicates local times and corresponding longitudes are mentioned on the top. At 0500 UT, the IMF is northward and hence considered as quiet time conditions and can be seen that different IMF-By orientations in Experiment 1, 2 and 3 do not show much differences, giving almost identical quite time drift patterns along with PRE in post-sunset hours (Figure 6i). At 0800 UT (Figure 6ii), the drift values are enhanced in both day and night sides compared to those during quiet times shown in Figure 6i. The dayside experienced larger upward drifts, whereas the night side experienced higher values of the downward drifts, which are consistent with the observations of Fejer et al. (2008). The PRE drifts are also high. The PRE peak drifts have increased to ~60 m/s compared to the quiet time value of ~20 m/s (Figure 6i). Note that here for most of the part, IMF-By = 0 case shows larger drift values, indicating that the presence of strong IMF-By reduces the drift amplitude; this feature we have noticed in the previous figures as well. Further, it can be observed that the change is not uniform over all LTs-stronger changes are seen at sunrise and sunset terminators, and least deviations are seen during daytime. At 1000 UT, soon after IMF-By transition and after ~4 h from southward turning of IMF-Bz, things

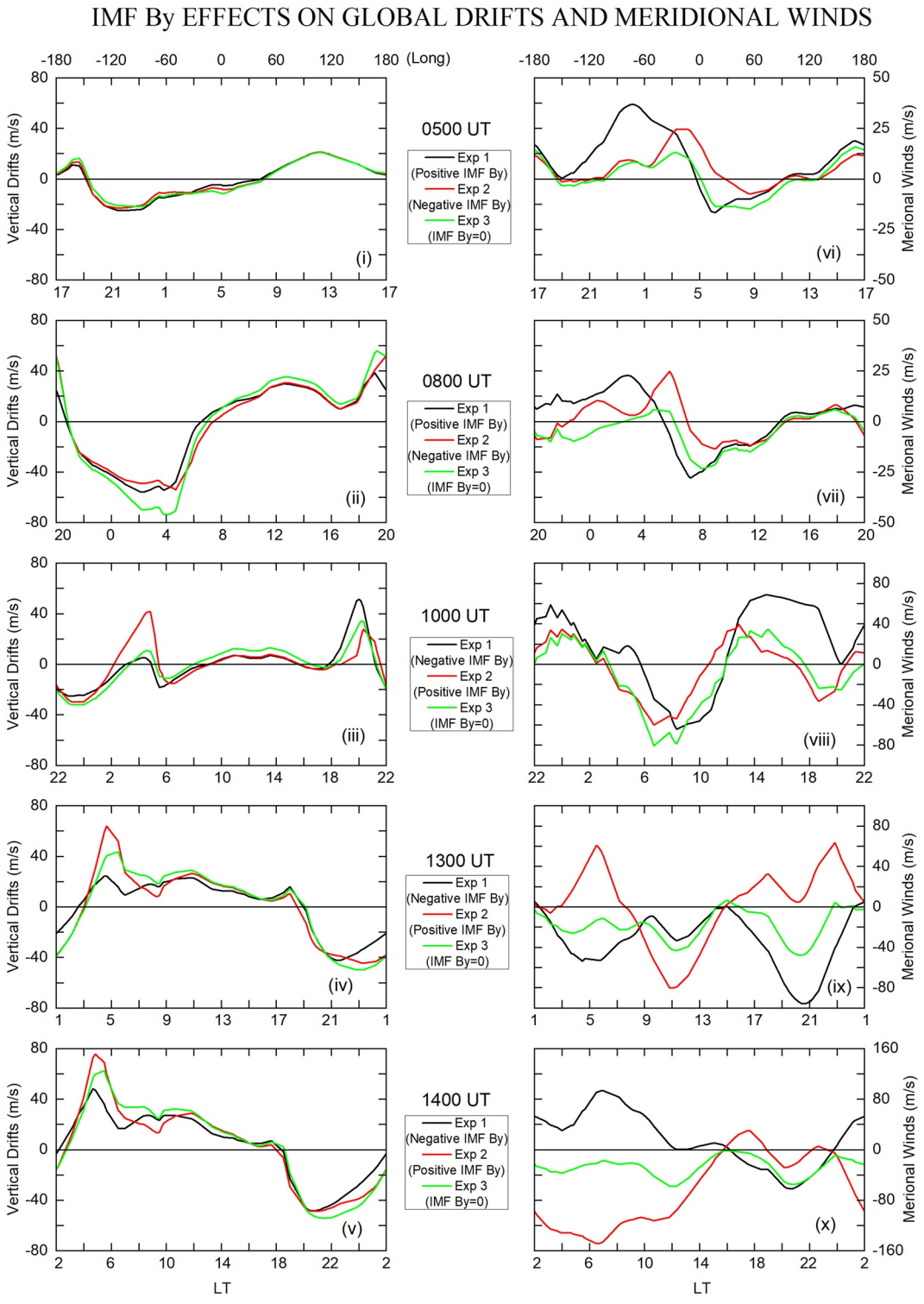

Figure 6. F-region vertical plasma drifts (left panels) over geomagnetic equator at different stages of IMF orientations (i–v) and corresponding meridional winds (right panels). Black, green and magenta curves represent results during Experiments 1, 2 and 3 respectively.

become more interesting. The morning pre-sunrise enhancement becomes pronounced. The drift values increase to positive values (upward) before sunrise followed by sharp decrease and then follow the typical daytime diurnal pattern with usual evening PRE before turning downward in the post sunset sector. This pattern with morning PRE is seen in all three curves, that is, appearance of morning PRE is evident even during zero IMF-By conditions, suggesting morning PRE is not due to IMF-By, and rather it is related to DD effects prevailed after about 3 h from the southward turning of IMF. However interestingly, the polarity of IMF-By seems to modify the DD effects, particularly during morning and evening PREs. Though the previous observation of higher drift values for IMF-By = 0 still hold during the day, the polarity of IMF-By seems to modulate the PRE peak values considerably. A strongly positive IMF-By seems to intensify the morning PRE and weaken the evening PRE compared to IMF-By = 0 condition. A strongly negative IMF-By acts just opposite. The increase (decrease) in the morning (evening) PRE over zero IMF-By values is ∼30 m/s (∼5 m/s) during positive IMF-By. Whereas during negative IMF-By, the decrease (increase) in the morning (evening) PRE is ∼5 m/s (∼20 m/s). It is important to note that the enhancement of morning PRE because of positive IMF-By explains the exception of higher drifts at 240°E and 270°E in Figures 4ix and 4x, whereas the drifts of morning PRE decreases in Figures 3ix and 3x during negative IMF-By. Although the evening PRE is strong at 1000 UT, it is weaker than that at 0800 UT for IMF-By = 0 and positive conditions. For negative IMF-By case, the evening PRE is stronger at 1000 UT. At later two time instances of 1300 UT and 1400 UT, the morning PRE gets more intensified, whereas the evening PRE gets further weakened. It is noted that the morning PRE maintains the same pattern of IMF-By polarity seen at 1000 UT (that is stronger drifts during positive IMF-By and weaker during negative IMF-By). Evening PRE also exhibits similar patterns as that at 1000 UT, although the differences are very small. The plots from 1000–1400 UT shown here exhibit a very strong morning PRE and suppressed evening PREs, which may be due to increasing effects of DD. To investigate further to understand the role of DD, equatorward meridional winds at these times are also looked into. Figures 6vi–6x show the winds corresponding to the drifts shown in Figures 6i–6v. A one to one correlation with meridional winds were difficult to make. Broadly, it can be seen that the meridional winds show roughly similar amplitudes at 0500 and 0800 UT (Figures 6vi and 6vii) but are largely intensified from 1000 UT onwards indicating strengthening of DD winds after few hours from storm commencement. At later times, the phases and amplitudes evolved rapidly (Figures 6ix and 6x). The most interesting feature from meridional wind observations are the opposite polarity of winds for opposite polarity of IMF-By from few hours after IMF-By transition.

5. Discussion and Summary

The effects of IMF-By on low latitude storm time ionospheric electrodynamics is a very obscure, rarely observed and addressed subject. Many previous studies (e.g., Ruohoniemi & Greenwald, 2005; Tenfjord et al., 2015; Yamazaki et al., 2015) have established that IMF-By causes substantial changes in the high latitude convection patterns, winds, thermospheric densities, induced By component in the closed magnetosphere and hemispheric asymmetries. In the present work, we have designed special experiments using TIEGCM model to understand the effect of IMF-By transition and polarity near equator that is, far beyond polar regions, during various stages of the geomagnetic storm. Perhaps there are other GCMs available, which can consider more realistic high latitude inputs (such as potential and electron precipitation etc.) through coupled MHD model, whereas TIEGCM utilizes empirical conductance calculations. The method used in the model to calculate the merging of high latitude potential with low to middle latitude wind dynamo potential is preliminary. Though the hemispherical asymmetries at low to middle latitudes are taken into account in TIEGCM, the asymmetries at high latitudes are not considered appropriately. Here, we have shown that TIEGCM responds to the IMF changes. However, the presented results should be treated with caution in the light of model limitations. In future, it would be interesting to run the simulations with similar IMF changes considered here using MHD coupled GCMs.

The designed numerical experiments consist of turning of IMF-Bz from northward to southward and remains southward for ∼9 h, thus creating geomagnetic storm kind of situation. PPEF effects are expected just after the onset of the storm and DD effects may exist after ∼2–3 h from the storm onset. With this background, the IMF-By component is varied from positive to negative in the first experiment, negative to positive in the second experiment and kept zero throughout the simulation in the third experiment. The

IMF-By changes are imposed after 3 h from the southward turning of the IMF. In order to bring out the relatively subtle effects of IMF-By at equator if any, we have used stronger amplitudes (20 nT) of IMFs, which normally occurs during major geomagnetic storms. Thus, the present work helps in understanding the effects of IMF-By polarities during various phases of the storm. We have designed the simulations to examine (a) whether non-zero IMF-By component alters the PPEF over equator, (b) if yes, what is the type of effect? - Does it enhance or reduce the PPEF effect? (c) Does this effect on PPEF vary with local time? (d) Does it depend on the IMF-By polarity? (e) Does the change in polarity that is, IMF-By transition affect the vertical drifts near equator? (f) Whether non-zero IMF-By component alters the DD effects, (g) Does the IMF-By effect on DDEF vary with local time? (h) Does the effect on DD depend on IMF-By polarity? (i) Does the IMF-By effect depend on the IMF-Bz orientation? The results from this study reveal that the IMF-By affects the equatorial ionospheric electrodynamics only during southward IMF and has negligible effects during northward IMF.

Our simulation results show that IMF-By plays role in reducing the prompt penetration electric fields over equator during the main phase of the storm, which is in accordance with the observations of Mannucci et al. (2014). It also shows that the IMF-By effects are considerable near the terminators, which is consistent with the observations by Chakrabarty et al. (2017). Here it is observed that the plasma drifts do not have dependence on the polarity of IMF-By during PPEF effects. Mannucci et al. (2014) examined the effects of the relative magnitudes of IMF-By with respect to IMF-Bz, (i.e., IMF-By > IMF-Bz and IMF-By < IMF-Bz). They have found that when IMF-Bz is less strong than IMF-By then the TEC build-up at low to mid latitudes is less significant. However, in our simulations both IMF-Bz and IMF-By are of the same magnitude, and yet reduced PPEF effects are observed with respect to zero IMF-By conditions. After ∼3 h from the storm onset when DD effects prevail, the morning PRE appears. However, the similar features are seen in all three experiments, suggesting that this feature is arising due to DD effects and not due to the IMF-By or its transition. Unfortunately, in our simulations IMF-By transitions are getting mixed up with DD effects, as we apply the IMF-By transition after ∼2.5 h from the onset. Therefore it is not really possible to examine the effects of IMF-By transitions independently. However, we have noticed that the evening PRE gets affected if it happens within 2 h from the IMF-By transition. In this time window, if the transition is from positive to negative then the PRE peaks are stronger and when transition is from negative to positive, then the PRE peak is smaller than no transition situation that is, zero IMF-By value.

During daytime, DD is expected to reduce the upward plasma drifts, and TIEGCM results are also in accordance with it. The IMF-By polarity seems to have varying influences on the morning and evening PREs. We found that a strongly positive IMF-By strengthens the morning PRE and weakens the evening PRE, with respect to zero IMF-By conditions. A strongly negative IMF-By just shows the reverse. Till date there are reports about the north-south asymmetry of the high-latitude plasma convection, wind and density caused by the IMF-By (Cowley, 1981; Förster et al., 2008; Østgaard et al., 2011; Reistad et al., 2016; Tanaka, 2001; Yamazaki et al., 2015). They have shown that the effects of positive IMF-By in the Northern hemisphere are similar to that of negative IMF-By in the southern hemisphere and vice versa. In the present paper, we report the dawn-dusk asymmetry of the equatorial plasma drifts due to IMF-By effects. The effects of positive IMF-By on morning PRE are similar to those of negative IMF-By on the evening PREs. This type of asymmetry near equator due to IMF-By effects has been reported here for the first time. Thus, the effect of positive/negative IMF-By near dawn has been found to be similar to the effect of negative/positive IMF-By near dusk terminator.

Now the next question arises: What is the physical mechanism behind such effects? The exact mechanism for various reported IMF-By effects on the Earth's electrodynamics is yet an evolving topic. There are several theories proposed to explain induced By component in the magnetosphere, asymmetrical loading of the lobes, the dynamics and configuration in the magnetosphere, ionospheric convection, hemispheric asymmetries of the high-latitude ion convection, wind, and densities, associated with IMF-By. The interaction between the solar wind and magnetosphere generates electric fields in the high-latitude ionosphere, which cause the ionospheric plasma to convect around the regions of positive and negative electric potentials, producing convection cells. The strength and orientation of the IMF strongly influence the ionospheric convection and associated thermospheric winds. The solar wind electric field given by Kan and Lee (1979) ($E_{SW} = |V_{sw}| B_T \sin^2(\theta/2)$, where clock angle, $\theta = \tan^{-1}$(IMF By, IMF Bz)), drives Region-1 currents

connecting solar wind with the Earth's magnetosphere-ionosphere. In the present three simulations at the time of PPEF, IMF-Bz was southward with the amplitude of 20 nT, but the amplitudes of IMF-By varied from zero, 20 nT and −20 nT. The corresponding clock angles would be 180°, 135° and −135°, which gives $\sin^2(\theta/2)$ factor as 1.0, 0.8535 and 0.8535 respectively. Thus, obviously the presence of IMF-By component would reduce the coupling by ∼15% compared to that of zero IMF-By conditions. And also, the polarity of IMF-By will not have any difference in the response. The modifications of the orientations of the convection cells due to IMF-By component are considerable near the terminators and hence can alter the PPEF significantly near the sunset/sunrise terminators.

Since thermospheric winds play important role in the ionospheric electrodynamics, it may provide some hint. Also, it is known that the electric fields of DD are generated due to world-wide changes in the thermospheric winds due to heating at high latitude, and the effects are large in the meridional wind component. Therefore, we examined the meridional winds evolved in our simulation experiments. Near storm onset, not much difference in the meridional winds was noticed. However after few hours, the F-region meridional winds at the equator are oppositely directed during positive and negative IMF-By conditions. This may suggest that during DDEFs, the meridional winds associated with different polarities of IMF-By are responsible for the observed effects on pre-sunrise and post-sunset PREs. Based on the thermospheric densities from CHAMP satellite, Kwak et al. (2009) found that the differences in the densities with respect to zero IMF-By conditions show significant enhancements in the dawn to early morning hours during negative IMF-By, but show reduced values in the dusk sector. For positive IMF-By, their observations were opposite in sign to those for negative IMF-By. These observations at high latitude may have some relation (though not obvious) with our simulation results of vertical plasma drifts and winds near pre-sunrise and post-sunset times. Kwak et al. (2009) too had attributed these observations to the thermospheric winds. They inferred that strong anticyclonic winds on the dusk side for negative IMF-By condition drive high neutral density on the dusk side of the polar cap; and for positive IMF-By, strong cyclonic winds on the dawn side drive low neutral density on the dawn side.

The results obtained from the present work are summarized below:

1. At the storm onset, a strong IMF-By reduces the vertical plasma drifts in the F-region over the equator during PPEF, indicating weaker prompt penetration electric fields over equator. The largest effects are observed near sunrise and sunset terminators.
2. After about 3 h from the southward turning of IMF-Bz, morning PRE appears and exhibits strong dependence on the polarity of IMF-By.
3. A strongly positive IMF-By strengthens the morning PRE and weakens the evening PRE, with respect to zero IMF-By conditions. A strongly negative IMF-By just shows the reverse. This suggests the dawn-dusk asymmetry of the equatorial plasma drifts due to IMF-By effects.
4. After few hours of IMF-By transitions, the meridional winds are oppositely directed during positive and negative IMF-By conditions. This may indicate the role of IMF-By polarity in the dynamics of storm time neutral atmosphere.
5. Within two hours of IMF-By transition, the effects of IMF-By polarity on evening PRE is observed. If the transition is from positive to negative (dusk to dawn-ward) then the PRE peaks are stronger and if the transition is from negative to positive (dawn to dusk-ward), then the PRE peak is smaller than no IMF-By transition situation.

Thus, the present study shows the importance of the polarity of IMF-By and their effects on ionospheric electrodynamics during storm time, particularly near morning and evening terminators and on the thermospheric meridional winds. Even though, we have not explicitly shown the results at mid-latitudes here, in the light of the above discussion, it can be expected that the IMF-By can influence the global storm time electrodynamics including the mid-latitudes, which are connected to both high and low latitudes. This study is the first effort to model the effects of IMF-By on equatorial storm time electrodynamics and with the new insight gained, it opens the door to a whole new understanding of storm time physics and its impact on global ionosphere-thermosphere. It is suggested that an altered potential distribution patterns associated with IMF-By conditions may modify the electric fields and neutral winds globally, which can produce the effects beyond polar latitudes even near equatorial region. The exact physical mechanism for the reduced penetration fields and dependence on IMF-By polarity needs to be investigated further using more careful

coordinated measurements and modeling. This newly gained knowledge could be a novel addition in improving the evaluation of space weather impacts globally.

Data Availability Statement

The TIEGCM model run results are available in the public domain in the CCMC website (https://ccmc.gsfc.nasa.gov/).

Acknowledgments
This work is carried out at IIG and supported by the Department of Science and Technology, Government of India. D. Hui thanks Ja Soon, A. M. Mendoza and other staffs from CCMC for support and cooperation on troubleshooting crashed runs for the models. G. Vichare thanks Astrid Maute for the discussions related to TIEGCM.

References

Blanc, M., & Richmond, A. D. (1980). The ionospheric disturbance dynamo. *Journal of Geophysical Research*, *85*, 1669–1686. https://doi.org/10.1029/ja085ia04p01669

Chakrabarty, D., Hui, D., Rout, D., Sekar, R., Bhattacharyya, A., Reeves, G. D., & Ruohoniemi, J. M. (2017). Role of IMF-By in the prompt electric field disturbances over equatorial ionosphere during a space weather event. *Journal of Geophysical Research: Space Physics*, *122*, 2574–2588. https://doi.org/10.1002/2016JA022781

Cowley, S. W. H. (1981). Magnetospheric asymmetries associated with the *y*-component of the IMF. *Planetary and Space Science*, *29*(1), 79–96. https://doi.org/10.1016/0032-0633(81)90141-0

Dickinson, R. E., Ridley, E. C., & Roble, R. G. (1981). A three-dimensional general circulation model of the thermosphere. *Journal of Geophysical Research*, *86*(A3), 1499–1512. https://doi.org/10.1029/JA086iA03p01499

Fejer, B. G., Jensen, J. W., & Su, S.-Y. (2008). Seasonal and longitudinal dependence of equatorial disturbance vertical plasma drifts. *Geophysical Research Letters*, *35*, L20106. https://doi.org/10.1029/2008GL035584

Förster, M., & Haaland, S. (2015). Interhemispheric differences in ionospheric convection: Cluster EDI observations revisited. *Journal of Geophysical Research: Space Physics*, *120*, 5805–5823. https://doi.org/10.1002/2014JA020774

Förster, M., Rentz, S., Köhler, W., Liu, H., & Haaland, S. E. (2008). IMF dependence of high-latitude thermospheric wind pattern derived from CHAMP cross-track measurements. *Annales Geophysicae*, *26*, 1581–1595. https://doi.org/10.5194/angeo-26-1581-2008

Gonzalez, W. D., Joselyn, J. A., Kamide, Y., Kroehl, H. W., Rostoker, G., Tsurutani, B. T., & Vasyliunas, V. M. (1994). What is a geomagnetic storm? *Journal of Geophysical Research*, *99*(A4), 5771–5792. https://doi.org/10.1029/93JA02867

Hagan, M. E., & Forbes, J. M. (2002). Migrating and nonmigrating diurnal tides in the middle and upper atmosphere excited by tropospheric latent heat release. *Journal of Geophysical Research*, *107*(D24), 4754. https://doi.org/10.1029/2001JD001236

Holappa, L., Asikainen, T., & Mursula, K. (2020). Explicit IMF B_y-dependence in geomagnetic activity: Modulation of precipitating electrons. *Geophysical Research Letters*, *47*, e2019GL086676. https://doi.org/10.1029/2019GL086676

Hui, D., & Vichare, G. (2019). Variable responses of equatorial ionosphere during undershielding and overshielding conditions. *Journal of Geophysical Research: Space Physics*, *124*, 1328–1342. https://doi.org/10.1029/2018ja025999

Iijima, T., Potemra, T. A., Zanetti, L. J., & Bythrow, P. F. (1984). Large-scale Birkeland currents in the dayside polar region during strongly northward IMF: A new Birkeland current system. *Journal of Geophysical Research*, *89*(A9), 7441–7452. https://doi.org/10.1029/JA089iA09p07441

Immel, T. J., Crowley, G., Hackert, C. L., Craven, J. D., & Roble, R. G. (2006). Effect of IMF By on thermospheric composition at high and middle latitudes: 2. Data comparisons. *Journal of Geophysical Research*, *111*, A10312. https://doi.org/10.1029/2005JA011372

Kan, J. R., & Lee, L. C. (1979). Energy coupling function and solar wind magnetosphere dynamo. *Geophysical Research Letters*, *6*(7), 577–580. https://doi.org/10.1029/GL006i007p00577

Kelley, M. C., & Makela, J. J. (2002). By dependent prompt penetrating electric fields at the magnetic equator. *Geophysical Research Letters*, *29*(7), 571–573. https://doi.org/10.1029/2001GL014468

Kelley, M. C., Nicolls, M. J., Anderson, D., Anghel, A., Chau, J. L., Sekar, R., et al. (2007). Multi-longitude case studies comparing the interplanetary and equatorial ionospheric electric fields using an empirical model. *Journal of Atmospheric and Terrestrial Physics*, *69*(10–11), 1174–1181. https://doi.org/10.1016/j.jastp.2006.08.014

Khurana, K. K., Walker, R. J., & Ogino, T. (1996). Magnetospheric convection in the presence of interplanetary magnetic field B_y: A conceptual model and simulations. *Journal of Geophysical Research*, *101*, 4907–4916. https://doi.org/10.1029/95JA03673

Kwak, Y.-S., & Richmond, A. D. (2014). Dependence of the high-latitude lower thermospheric wind vertical vorticity and horizontal divergence on the interplanetary magnetic field. *Journal of Geophysical Research: Space Physics*, *119*, 1356–1368. https://doi.org/10.1002/2013JA019589

Kwak, Y.-S., Richmond, A. D., Deng, Y., Ahn, B.-H., & Cho, K.-S. (2010). Sources of the high-latitude thermospheric neutral mass density variations. *Journal of Astronomy and Space Sciences*, *27*(4), 329–335. https://doi.org/10.5140/JASS.2010.27.4.329

Kwak, Y.-S., Richmond, A. D., Deng, Y., Forbes, J. M., & Kim, K.-H. (2009). Dependence of the high-latitude thermospheric densities on the interplanetary magnetic field. *Journal of Geophysical Research*, *114*, A05304. https://doi.org/10.1029/2008JA013882

Lei, J., Zhu, Q., Wang, W., Burns, A. G., Zhao, B., Luan, X., et al. (2015). Response of the topside and bottomside ionosphere at low and middle latitudes to the October 2003 superstorms. *Journal of Geophysical Research: Space Physics*, *120*(8), 6974–6986. https://doi.org/10.1002/2015JA021310

Mannucci, A. J., Crowley, G., Tsurutani, B. T., Verkhoglyadova, O. P., Komjathy, A., & Stephens, P. (2014). Interplanetary magnetic field by control of prompt total electron content increases during superstorms. *Journal of Atmospheric and Solar-Terrestrial Physics*, *115*, 7–16. https://doi.org/10.1016/j.jastp.2014.01.001

Maute, A. (2017). Thermosphere-ionosphere-electrodynamics general circulation model for the ionospheric connection explorer: TIEGCM-ICON. *Space Science Reviews*, *212*(1–2), 523–551. https://doi.org/10.1007/s11214-017-0330-3

Maute, A., Richmond, A. D., Lu, G., Knipp, D. J., Shi, Y., & Anderson, B. (2021). Magnetosphere-ionosphere coupling via prescribed field-aligned current simulated by the TIEGCM. *Journal of Geophysical Research: Space Physics*, *126*, e2020JA028665. https://doi.org/10.1029/2020JA028665

Newell, P. T., Sotirelis, T., Liou, K., Meng, C.-I., & Rich, F. J. (2007). A nearly universal solar wind-magnetosphere coupling function inferred from 10 magnetospheric state variables. *Journal of Geophysical Research*, *112*, A01206. https://doi.org/10.1029/2006JA012015

Nopper, R. W., & Carovillano, R. L. (1978). Polar-equatorial coupling during magnetically active periods. *Geophysical Research Letters*, *5*(8), 699–702. https://doi.org/10.1029/GL005i008p00699

Ohma, A., Østgaard, N., Reistad, J. P., Tenfjord, P., Laundal, K. M., Snekvik, K., et al. (2018). Evolution of asymmetrically displaced footpoints during substorms. *Journal of Geophysical Research: Space Physics*, *123*(10), 063. https://doi.org/10.1029/2018JA025869

Østgaard, N., Laundal, K. M., Juusola, L., Åsnes, A., Haaland, S. E., & Weygand, J. M. (2011). Interhemispherical asymmetry of substorm onset locations and the interplanetary magnetic field. *Geophysical Research Letters*, *38*, L08104. https://doi.org/10.1029/2011GL046767

Qian, L., Burns, A. G., Emery, B. A., Foster, B., Lu, G., Maute, A., et al. (2014). The NCAR TIE-GCM. In J. Huba, R. Schunk, & G. Khazanov (Eds.), *Modeling the ionosphere–thermosphere system* (pp. 73–84). https://doi.org/10.1002/9781118704417.ch7

Reistad, J. P., Østgaard, N., Tenfjord, P., Laundal, K. M., Snekvik, K., Haaland, S. E., et al. (2016). Dynamic effects of restoring footpoint symmetry on closed magnetic field lines. *Journal of Geophysical Research: Space Physics*, *121*, 5520–5536. https://doi.org/10.1002/2015JA022058

Richmond, A. D. (1995). Ionospheric electrodynamics using magnetic apex coordinates. *Journal of Geomagnetism and Geoelectricity*, *47*, 191–212. https://doi.org/10.5636/jgg.47.191

Richmond, A. D., Fang, T.-W., & Maute, A. (2015). Electrodynamics of the equatorial evening ionosphere: 1. Importance of winds in different regions. *Journal of Geophysical Research: Space Physics*, *120*, 2118–2132. https://doi.org/10.1002/2014JA020934

Richmond, A. D., Peymirat, C., & Roble, R. G. (2003). Long-lasting disturbances in the equatorial ionospheric electric field simulated with a coupled magnetosphere-ionosphere thermosphere model. *Journal of Geophysical Research*, *108*, 1118. https://doi.org/10.1029/2002JA009758

Richmond, A. D., Ridley, E. C., & Roble, R. G. (1992). A thermosphere/ionosphere general circulation model with coupled electrodynamics. *Geophysical Research Letters*, *19*(6), 601–604. https://doi.org/10.1029/92GL00401

Roble, R. G., Ridley, E. C., Richmond, A. D., & Dickinson, R. E. (1988). A coupled thermosphere/ionosphere general circulation model. *Geophysical Research Letters*, *15*(12), 1325–1328. https://doi.org/10.1029/GL015i012p01325

Rodrigues, F. G., Crowley, G., Heelis, R. A., Maute, A., & Reynolds, A. (2012). On TIE-GC simulation of equatorial plasma vortex. *Journal of Geophysical Research*, *117*, A05307. https://doi.org/10.1029/2011ja017369

Ruohoniemi, J. M., & Greenwald, R. A. (2005). Dependencies of high-latitude plasma convection: Consideration of interplanetary magnetic field, seasonal, and universal time factors in statistical patterns. *Journal of Geophysical Research*, *110*, A09204. https://doi.org/10.1029/2004JA010815

Shiokawa, K., Lu, G., Otsuka, Y., Ogawa, T., Yamamoto, M., Nishitani, N., & Sato, N. (2007). Ground observation and AMIE-TIEGCM modeling of a storm-time traveling ionospheric disturbance. *Journal of Geophysical Research*, *112*, A05308. https://doi.org/10.1029/2006JA011772

Tanaka, T. (2001). Interplanetary magnetic field B_y and auroral conductance effects on high-latitude ionospheric convection patterns. *Journal of Geophysical Research*, *106*(A11), 24505–24516. https://doi.org/10.1029/2001JA900061

Tenfjord, P., Østgaard, N., Haaland, S., Snekvik, K., Laundal, K. M., Reistad, J. P., et al. (2018). How the IMF B_y induces a local B_y component during northward IMF B_z and characteristic timescales. *Journal of Geophysical Research: Space Physics*, *123*, 3333–3348. https://doi.org/10.1002/2018JA025186

Tenfjord, P., Østgaard, N., Snekvik, K., Laundal, K. M., Reistad, J. P., Haaland, S., & Milan, S. E. (2015). How the IMF By induces a By component in the closed magnetosphere and how it leads to asymmetric currents and convection patterns in the two hemispheres. *Journal of Geophysical Research: Space Physics*, *120*, 9368–9384. https://doi.org/10.1002/2015JA021579

Vichare, G., & Richmond, A. D. (2005). Simulation study of the longitudinal variation of evening vertical ionospheric drifts at the magnetic equator during equinox. *Journal of Geophysical Research*, *110*, A05304. https://doi.org/10.1029/2004JA010720

Wang, W., Lei, J., Burns, A. G., Wiltberger, M., Richmond, A. D., Solomon, S. C., et al. (2008). Ionospheric electric field variations during a geomagnetic storm simulated by a coupled magnetosphere ionosphere thermosphere (CMIT) model. *Geophysical Research Letters*, *35*, L18105. https://doi.org/10.1029/2008GL035155

Weimer, D. R. (2005). Improved ionospheric electrodynamic models and application to calculating Joule heating rates. *Journal of Geophysical Research*, *110*, A05306. https://doi.org/10.1029/2004JA010884

Wygant, J. R., Torbert, R. B., & Mozer, F. S. (1983). Comparison of S3-3 polar cap potential drops with the interplanetary magnetic field and models of magnetopause reconnection. *Journal of Geophysical Research*, *88*, 5727–5735. https://doi.org/10.1029/ja088ia07p05727

Yamazaki, Y., Kosch, M. J., & Sutton, E. K. (2015). North-south asymmetry of the high latitude thermospheric density: IMF By effect. *Geophysical Research Letters*, *42*, 225–232. https://doi.org/10.1002/2014GL062748